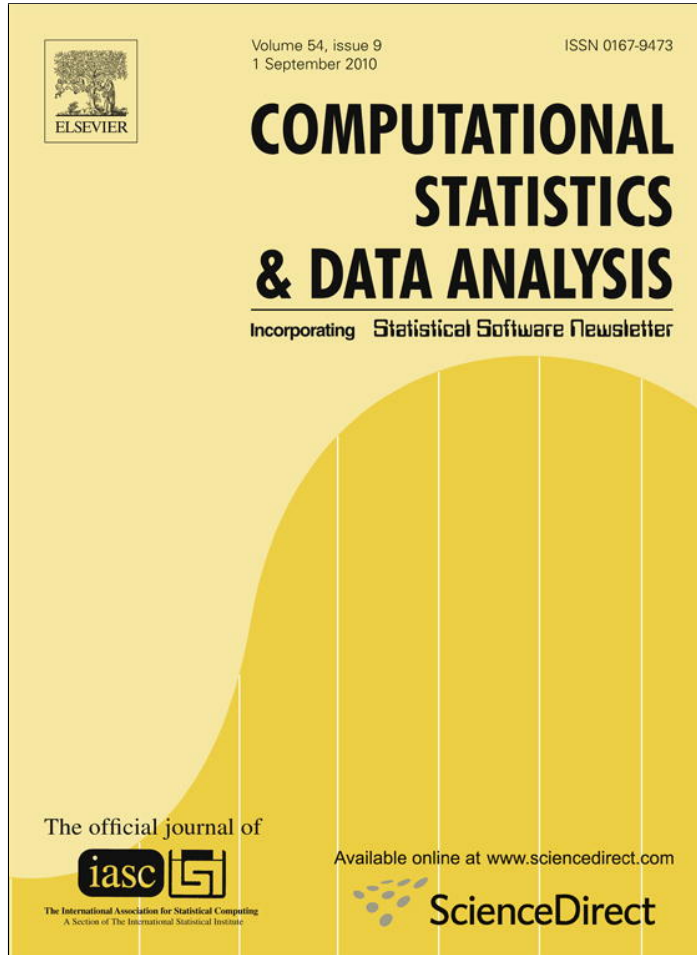


Provided for non-commercial research and education use.
Not for reproduction, distribution or commercial use.



This article appeared in a journal published by Elsevier. The attached copy is furnished to the author for internal non-commercial research and education use, including for instruction at the authors institution and sharing with colleagues.

Other uses, including reproduction and distribution, or selling or licensing copies, or posting to personal, institutional or third party websites are prohibited.

In most cases authors are permitted to post their version of the article (e.g. in Word or Tex form) to their personal website or institutional repository. Authors requiring further information regarding Elsevier's archiving and manuscript policies are encouraged to visit:

<http://www.elsevier.com/copyright>



Contents lists available at ScienceDirect

Computational Statistics and Data Analysis

journal homepage: www.elsevier.com/locate/csda

A new image segmentation algorithm with applications to image inpainting

Silvia Ojeda^a, Ronny Vallejos^{b,*}, Oscar Bustos^a^a Facultad de Matemática, Astronomía y Física, Universidad Nacional de Córdoba, Haya de la Torre y Medina Allende S/N, Código Postal 5000, Córdoba, Argentina^b Departamento de Matemática, Universidad Técnica Federico Santa María, Casilla 110-V, Valparaíso, Chile

ARTICLE INFO

Article history:

Received 24 September 2009

Received in revised form 26 March 2010

Accepted 27 March 2010

Available online 8 April 2010

Keywords:

Image segmentation

Border detection

Spatial AR models

Robust estimators

Image inpainting

ABSTRACT

This article describes a new approach to perform image segmentation. First an image is locally modeled using a spatial autoregressive model for the image intensity. Then the residual autoregressive image is computed. This resulting image possesses interesting texture features. The borders and edges are highlighted, suggesting that our algorithm can be used for border detection. Experimental results with real images are provided to verify how the algorithm works in practice. A robust version of our algorithm is also discussed, to be used when the original image is contaminated with additive outliers. A novel application in the context of image inpainting is also offered.

© 2010 Elsevier B.V. All rights reserved.

1. Introduction

During the past decades, image segmentation and edge detection have been two important and challenging topics. The main idea is to produce a partition of an image such that each category or region is homogeneous with respect to some measures. The processed image can be useful for posterior image processing treatments. Many techniques have been studied in this field, from different perspectives, and several different disciplines have been involved. For example, unsupervised clustering techniques (Jain et al., 1999), and morphological multifractal estimation for image segmentation (Xia et al., 2006) have been used, among others.

Two-dimensional autoregressive (AR-2D) models are one way to represent the image intensity of a given picture by a small number of parameters. This class of models, pioneered by Whittle (1954), has been studied in several different disciplines. Kashyap and Eom (1988) developed an image restoration algorithm based on robust estimation of a two-dimensional autoregressive model. Cariou and Chehdi (2008) used a two-dimensional autoregressive model to perform unsupervised texture segmentation. Allende et al. (2001) generalized the algorithm proposed by Kashyap and Eom (1988), using the generalized M estimators to deal with the effect caused by additive contamination. Later on, Ojeda et al. (2002) developed robust autocovariance (RA) estimators for AR-2D processes. Several theoretical contributions have been suggested in the literature. For example, Baran et al. (2004) investigated asymptotic properties of a nearly unstable sequence of stationary spatial autoregressive processes. Other contributions and applications of spatial autoregressive moving average (ARMA) processes can be found in Tjostheim (1978), Guyon (1982), Basu and Reinsel (1993), Martin (1996), Francos and Friedlander (1998), Illig and Truong-Van (2006).

In this paper we focus our attention on segmentation and edge detection of texture images. A new image segmentation algorithm that highlights the edges of an image is described. The algorithm consists in locally fitting a two-dimensional

* Corresponding author. Tel.: +56 32 2508169; fax: +56 32 2508322.

E-mail address: ronny.vallejos@usm.cl (R. Vallejos).

autoregressive model to the original image. That is, the original image is divided into small regions and an AR-2D model is fitted to each of these regions. A new image is generated, putting together all images generated by fitting the local AR-2D models to the original one. Then the autoregressive residual image is computed. As a result, the original borders are highlighted and the areas with different textures are noticed. One advantage of our algorithm is its simplicity, since in practice a large class of images can be well represented by AR-2D models with less than four parameters. The fitted AR-2D model plays an important role in the segmentation process because the quality of the fitted model significantly affects the segmentation results.

Numerical studies with real images are offered to inspect the advantages and limitations of our proposal. Several images were processed to gain a better insight into the performance of the algorithm. In each case, AR-2D models were used to represent the original patterns considering least squares estimation for the parameters. The same algorithm is studied when the image is blurred by additive contamination. In this case it is well known that traditional methods of estimation of AR-2D models yield estimators that are highly sensitive to outliers. The effect on the segmentation produced by the proposed algorithm is discussed. We also present experiments in which robust estimation has been used instead of traditional least squares (LS) and maximum likelihood (ML) estimations.

Inpainting is a technique to reconstruct damaged or missed portions of an image. A novel application using real images is shown in this framework. Our algorithm is able to detect some patterns on images that have been previously processed by inpainting techniques to fill certain small image gaps, highlighting the gaps or imperfections existing in the original image.

The paper is organized as follows. In Section 2, we give an overview of the spatial AR processes. In Section 3, the main robust estimation methods are reviewed. Section 4 describes the new image segmentation algorithm. In Section 5, a simulation experiment is developed to illustrate the segmentation procedure. In Section 6, the performance of our algorithm is inspected under additive contamination. Section 7 presents an application of our algorithm for image inpainting. We conclude and present possible extensions of this work in Section 8.

2. The spatial ARMA processes

In order to represent images using models that are statistically treatable, three classes of model have been proposed. Whittle (1954) studied simultaneous autoregressive (AR) models; Besag (1974) introduced conditional autoregressive models. Moving average (MA) models were studied by Haining (1978).

Spatial autoregressive moving average (ARMA) processes have also been studied in the context of random fields indexed over \mathbb{Z}^d , $d \geq 2$, where \mathbb{Z}^d is endowed with the usual partial order; that is; for $s = (s_1, s_2, \dots, s_d)$, $u = (u_1, u_2, \dots, u_d)$ in \mathbb{Z}^d , $s \leq u$ if, for $i = 1, 2, \dots, d$, $s_i \leq u_i$. For $a, b \in \mathbb{Z}^d$, such that $a \leq b$ and $a \neq b$, we define

$$\begin{aligned} S[a, b] &= \{x \in \mathbb{Z}^d \mid a \leq x \leq b\}, \\ S\langle a, b \rangle &= S[a, b] \setminus \{a\}. \end{aligned}$$

Following Tjostheim (1978), a random field $(X_s)_{s \in \mathbb{Z}^d}$ is said to be a spatial ARMA(p, q) with parameters $p, q \in \mathbb{Z}^d$ if it is weakly stationary and satisfies the equation

$$X_s - \sum_{j \in S\langle 0, p \rangle} \phi_j X_{s-j} = \epsilon_t + \sum_{k \in S\langle 0, q \rangle} \theta_k \epsilon_{s-k}, \quad (1)$$

where $(\phi_j)_{j \in S\langle 0, p \rangle}$ and $(\theta_k)_{k \in S\langle 0, q \rangle}$ denote, respectively, the autoregressive and moving average parameters with $\phi_0 = \theta_0 = 1$, and $(\epsilon_s)_{s \in \mathbb{Z}^d}$ denotes a family of independent and identically distributed (iid) centered random variables with variance σ^2 . Notice that, if $p = 0$, the sum over $S\langle 0, p \rangle$ is supposed to be zero, and the process is called a spatial autoregressive AR(p) random field. Similarly if $q = 0$ the process is called an MA(q) random field.

The ARMA random field is called causal if it has the following unilateral representation:

$$X_s = \sum_{j \in S[0, \infty]} \psi_j \epsilon_{s-j},$$

with $\sum_j |\psi_j| < \infty$.

In practice, spatial ARMA models have been used in several applications in different fields. For example, spatial ARMA models were used to analyze yield trials in the context of incomplete block designs (Grondona et al., 1996). See also Cullis and Glesson (1991). Basu and Reinsel (1993) studied the spatial unilateral first-order ARMA model to examine regression models with spatially correlated errors. Extensions of the theory developed for time series to spatial ARMA models can be found in Tjostheim (1978), Guo and Billard (1998), Choi (2000), and Baran et al. (2004).

As an example, consider a particular case of model (1) when $d = 2$ and $p = (1, 1)$. This model is called a first-order autoregressive process. Note that $S\langle(0, 0), (1, 1)\rangle = \{(0, 1), (1, 0), (1, 1)\}$ and the model is of the form

$$X_{i,j} = \phi_{1,0} X_{i-1,j} + \phi_{0,1} X_{i,j-1} + \phi_{1,1} X_{i-1,j-1} + \epsilon_{i,j}. \quad (2)$$

The correlation structure of a process like (2) was investigated by Basu and Reinsel (1993). They obtained conditions to guarantee the stationarity of the process. In that case, a multinomial expansion for the function $(1 - \phi_{1,0}z_1 - \phi_{0,1}z_2 - \phi_{1,1}z_1z_2)^{-1}$ can be used to get a causal representation of the process that allows us to compute the moments of $X_{i,j}$.

In the literature there exist several prediction windows that can be considered in the definition of a spatial ARMA process. For example, Kashyap and Eom (1988) used a finite subset N_1 of the non-symmetrical half plane Ω_- given by

$$\Omega_- = \{(i, j) : (i = 0 \text{ and } j < 0) \text{ or } (i < 0 \text{ and } j \text{ is arbitrary})\}.$$

A strong causal prediction neighborhood was suggested by Guyon (1993); this prediction window will be used in Section 3. A complete treatment of the prediction window for spatial ARMA models and examples can be found in Guyon (1995) and Bustos et al. (2009b).

3. Robust parametric estimation

Innovation outliers (IOs) and additive outliers (AOs) are well known in time series (Fox, 1972). The same notion of data contamination has been studied for spatial processes. A more recent discussion about types of contamination in time series can be found in Chang et al. (1988) and Chen and Lui (1993). The definitions of outliers have been extended to a multivariate framework and the effects of multivariate outliers on the joint and marginal models have been examined by Tsay et al. (2000).

It is well known that ML estimators are very sensitive to outliers (Martin, 1980). This fostered the introduction of several alternative estimators to attenuate the impact of contaminated observations on the estimators. Most of these proposals are natural extensions of robust estimators studied in time series.

Robust estimators have been defined for models containing a finite number of parameters. Here we use model (2) to describe the well-known robust estimators; however, a more general treatment for AR and MA models can be found in Kashyap and Eom (1988), Allende et al. (2001), Ojeda et al. (2002), Vallejos and Garcia-Donato (2006), and Bustos et al. (2009a).

Notice that model (2) can be rewritten in the linear model form:

$$X_{i,j} = \boldsymbol{\phi}^T Z_{i,j} + \epsilon_{i,j},$$

where $\boldsymbol{\phi}^T = (\phi_{1,0}, \phi_{0,1}, \phi_{1,1})$ is a parameter vector and $Z_{i,j}^T = (X_{i-1,j}, X_{i,j-1}, X_{i-1,j-1})$. To obtain the LS estimator of $\boldsymbol{\phi}$ we need to minimize the function

$$\sum_{i,j} [X_{i,j} - \boldsymbol{\phi}^T Z_{i,j}]^2$$

with respect to $\boldsymbol{\phi}$. Similarly, the class of M estimators for causal autoregressive processes (Kashyap and Eom, 1988), defined by minimizing the function of a finite sample of observations

$$Q(\boldsymbol{\phi}, \sigma) = \sum_{i,j} \left[\rho \left(\frac{X_{i,j} - \boldsymbol{\phi}^T Z_{i,j}}{\sigma} \right) + \frac{1}{2} \right] \sigma, \quad (3)$$

is robust for innovation outliers, when the function ρ is a differentiable function, convex, symmetric with respect to the origin, with bounded derivative, and such that $\rho(0) = 0$. However, the M estimators are very sensitive when the process is contaminated with additive outliers. This suggested the introduction of other robust estimators able to lessen the effects of additive outliers. Allende et al. (2001) developed generalized M (GM) estimators for spatial AR processes. A GM estimator of $\boldsymbol{\phi}$ is the solution to the problem of minimizing the non-quadratic function defined by

$$Q(\boldsymbol{\phi}, \sigma) = \sum_{i,j} l_{ij} t_{ij} \left[\rho \left(\frac{X_{i,j} - \boldsymbol{\phi}^T Z_{i,j}}{l_{ij}\sigma} \right) + \frac{1}{2} \right] \sigma,$$

where ρ is as in (3), and t_{ij} and l_{ij} are weights corresponding to the respective $Z_{i,j}$.

Alternatively, Ojeda et al. (2002) introduced robust autocovariance (RA) estimators for spatial autoregressive processes. This estimator was first introduced by Bustos and Yohai (1986) for models used in time series.

Let X be a zero-mean AR-2D process described by the equation

$$X_{m,n} - \sum_{k,l \in S\langle 0,p \rangle} \phi_{k,l} X_{m-k,n-l} = \epsilon_{m,n}, \quad (4)$$

where $\epsilon_{m,n}$ is a sequence of iid random variables with $\text{Var}(\epsilon_{m,n}) = \sigma^2$. Assume that X is observed on a strongly causal squared window of order M , $W_M = \{(k, l) \in S : 0 \leq k, l \leq M\}$, where S is an infinite strong causal prediction neighborhood. Let us define $W_M \setminus S\langle 0, p \rangle = \{(m, n) \in W_M : [(m, n) - p] \in W_M\}$. The residual of order (m, n) in $\boldsymbol{\phi}$ of X is

$$r(m, n) = \begin{cases} - \sum_{k,l \in T'} \phi_{k,l} X_{m-k,n-l}, & (m, n) \in (W_M \setminus S\langle 0, p \rangle) \\ 0, & \text{otherwise,} \end{cases} \quad (5)$$

where $T' = S(0, p] \cup \{(0, 0)\}$ and $\phi_{0,0} = -1$. In particular, for $p = (1, 1)$, we define the coefficients

$$p_\phi(k, l, r) = \frac{(k+l+r)!}{k! l! r!} \phi_{1,0}^k \phi_{0,1}^l \phi_{1,1}^r;$$

then the RA estimator $\hat{\phi}$ of ϕ is defined by the following equations:

$$\sum_{k,l,r=0}^{\infty} p_\phi(k, l, r) \sum_{(m,n) \in (W_M \setminus S(0, (1, 1))]} \eta \left(\frac{r(m, n)}{\hat{\sigma}}, \frac{r(m-i-k-r, n-j-l-r)}{\hat{\sigma}} \right) = 0, \quad (6)$$

$$\sum_{(m,n) \in (W_M \setminus S(0, (1, 1))]} \psi \left(\frac{r(m, n)}{\hat{\sigma}} \right) = 0, \quad (7)$$

where $\hat{\sigma}$ is estimated independently by

$$\hat{\sigma} = \text{Med}(|r(m, n)| : (m, n) \in (W_M \setminus S(0, (1, 1))))/0.6745, \quad (8)$$

η is a continuous, bounded and odd function in two variables and $0.6745 = \text{Med}(|Y|)$, where Y is a standard normal random variable. Two possible choices for η have been suggested in the literature (see Bustos et al., 2009b)

4. The new algorithm

In this section we present two algorithms. The first one produces a local approximation of images by using unilateral AR-2D processes. The second one is the new segmentation algorithm.

The first algorithm is based on the fact that it is possible to represent any image by using unilateral AR-2D processes. This image is called a local AR-2D approximated image by using blocks.

Let

$$Z = [Z_{m,n}]_{0 \leq m \leq M-1, 0 \leq n \leq N-1},$$

be the original image, and let

$$X = [X_{m,n}]_{0 \leq m \leq M-1, 0 \leq n \leq N-1},$$

where, for all $0 \leq m \leq M-1, 0 \leq n \leq N-1$,

$$X_{m,n} = Z_{m,n} - \bar{Z},$$

and \bar{Z} is the mean of Z . As an example, consider the approximated image Y of Z based on a causal AR-2D process of the form

$$Y_{i,j} = \phi_1 Y_{i-1,j} + \phi_2 Y_{i,j-1} + \varepsilon_{i,j},$$

where $(i, j) \in \mathbb{Z}^2$ and $(\varepsilon_{i,j})_{(i,j) \in \mathbb{Z}^2}$ is a Gaussian white noise.

Let $4 \leq k \leq \min(M, N)$. For simplicity we shall consider from now on that the images to be processed (Z and X) are arranged in such a way that the number of columns minus one and the number of rows minus one are multiples of $k-1$; that is,

$$Z = [Z_{m,n}]_{0 \leq m \leq M'-1, 0 \leq n \leq N'-1},$$

$$X = [X_{m,n}]_{0 \leq m \leq M'-1, 0 \leq n \leq N'-1},$$

where $M' = \lceil \frac{M-1}{k-1} \rceil (k-1) + 1$, $N' = \lceil \frac{N-1}{k-1} \rceil (k-1) + 1$. For all $i_b = 1, \dots, \lceil \frac{M-1}{k-1} \rceil$, and for all $j_b = 1, \dots, \lceil \frac{N-1}{k-1} \rceil$, we define the $(k-1) \times (k-1)$ block (i_b, j_b) of the image X by

$$B_X(i_b, j_b) = [X_{r,s}]_{(k-1)(i_b-1)+1 \leq r \leq (k-1)i_b, (k-1)(j_b-1)+1 \leq s \leq (k-1)j_b}.$$

The $M' \times N'$ approximated image \hat{X} of X is provided by the following algorithm.

Algorithm 1. For each block $B_X(i_b, j_b)$:

1. Compute the least square estimators $\hat{\phi}_1(i_b, j_b), \hat{\phi}_2(i_b, j_b)$ of ϕ_1 and ϕ_2 corresponding to the block $B_X(i_b, j_b)$ extended to

$$B'_X(i_b, j_b) = [X_{r,s}]_{(k-1)(i_b-1) \leq r \leq (k-1)i_b, (k-1)(j_b-1) \leq s \leq (k-1)j_b}.$$

2. Let \hat{X} be defined on the block $B_X(i_b, j_b)$ by

$$\hat{X}_{r,s} = \hat{\phi}_1(i_b, j_b) X_{r-1,s} + \hat{\phi}_2(i_b, j_b) X_{r,s-1},$$

where $(k-1)(i_b-1) + 1 \leq r \leq (k-1)i_b$ and $(k-1)(j_b-1) + 1 \leq s \leq (k-1)j_b$.

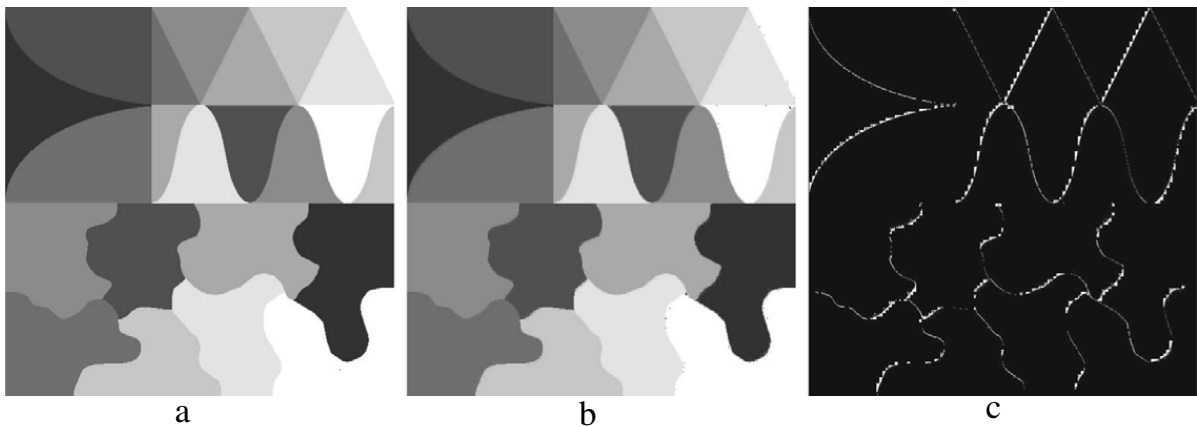


Fig. 1. (a) Original image; (b) Image generated by an AR-2D model; (c) Residual autoregressive image yielded by Algorithm 2.

Then the approximated image \widehat{Z} of the original image Z is

$$\widehat{Z}_{m,n} = \widehat{X}_{m,n} + \bar{Z}, \quad 0 \leq m \leq M' - 1, 0 \leq n \leq N' - 1.$$

Now we describe the segmentation algorithm based on a generated image from Algorithm 1. Assume that an original image Z is available.

Algorithm 2 (Segmentation Algorithm).

1. Use Algorithm 1 to generate an approximated image \widehat{Z} of Z .
2. Compute the residual autoregressive image $Z - \widehat{Z}$.

Notice from step 2 in Algorithm 1 that the least squares estimators for the parameters of the AR-2D process have been used. However, Algorithm 2 is not necessarily dependent on this estimation method. Eventually, other estimation methods that are able to reproduce well the homogeneous parts of the image, highlighting the borders and boundaries, could be used to generate the fitted image. In particular, robust methods of estimation will be used in the next section when the original image is contaminated.

5. Numerical experiments

In this section, we present numerical experiments that illustrate the performance of Algorithm 2. The images considered in the experiment were taken from the USC-SIPI image database <http://sipi.usc.edu/database/>. Fig. 1(a) shows an original image of size 512×512 . Fig. 1(b) shows the image produced by Algorithm 1 using a moving window of size 7×7 . In Fig. 1(c), we display the residual autoregressive image yielded by Algorithm 2. Notice from Fig. 1(b) that the local approximated image is visually very similar to the original one. This is an interesting feature of the AR-2D model. A wide class of images can be well represented by the images generated by Algorithm 1 in which the AR-2D model is fitted to 7×7 blocks and then the whole original image is reproduced by putting all generated local images together. This form of image filtering based on the estimation of spatial autoregressive models has recently been studied by Bustos et al. (2009b). The mean square error (MSE) has been used to quantify the difference between the original and final images. In practice, the fitted spatial autoregressive model works well for a large class of images. However, Algorithm 1 does not work well, producing a large MSE for images affected by a strong multiplicative speckle noise.

In Figs. 2 and 3, four images (texmos, auto, mandrill, and Lenna) of size 512×512 have been considered. These images were processed by Algorithm 2 with different moving window sizes. Images (b)–(h) were produced using a moving window size of 8×8 , 16×16 , 32×32 , 64×64 , 128×128 , 256×256 , and 512×512 , respectively. We observe that the segmentation yielded by the proposed method strongly depends on the size of the moving window. The residual autoregressive images generated with a small window size seems to highlight the borders less than the images generated with a large window size. Moreover, the best performance is obtained when using a moving window size of 512×512 . That is, the fitted autoregressive image was generated using only one model. The same pattern is observed in all processed images. One possible reason to explain this behavior is that a small window size is associated to a large number of AR models fitted to the original image. This produces a better local approximation, and hence the patterns in the fitted image are very well represented. The residual autoregressive image will not highlight the original borders and boundaries because both images are too similar. However, when the window size is large, the fitted image is a poor representation of the original patterns; thus the residual autoregressive image captures the large deviations from the original textures that are located at the borders or those areas that divide the original image in several regions which usually show a variety of different textures. As a result, and based on our experience dealing with Algorithm 2, we recommend using the maximum possible size for the moving window. This

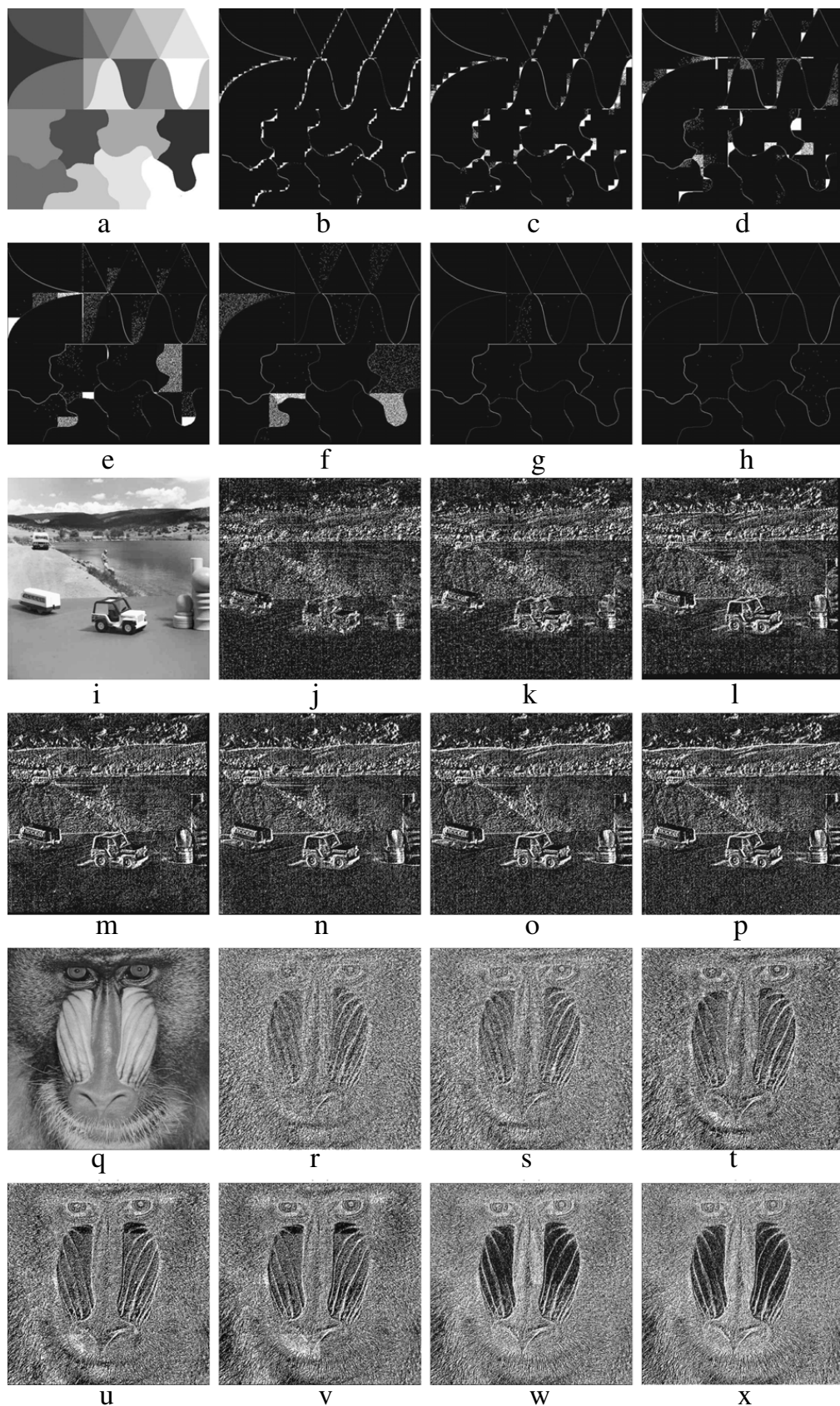


Fig. 2. Original images ((a), (i) and (q)). Segmentation produced by Algorithm 2 with window size 8×8 , 16×16 , 32×32 , 64×64 , 128×128 , 256×256 , and 512×512 , respectively.

optimum window size may be different for image filtering purposes. In that case, a small window size is required to obtain appropriate local approximated images.

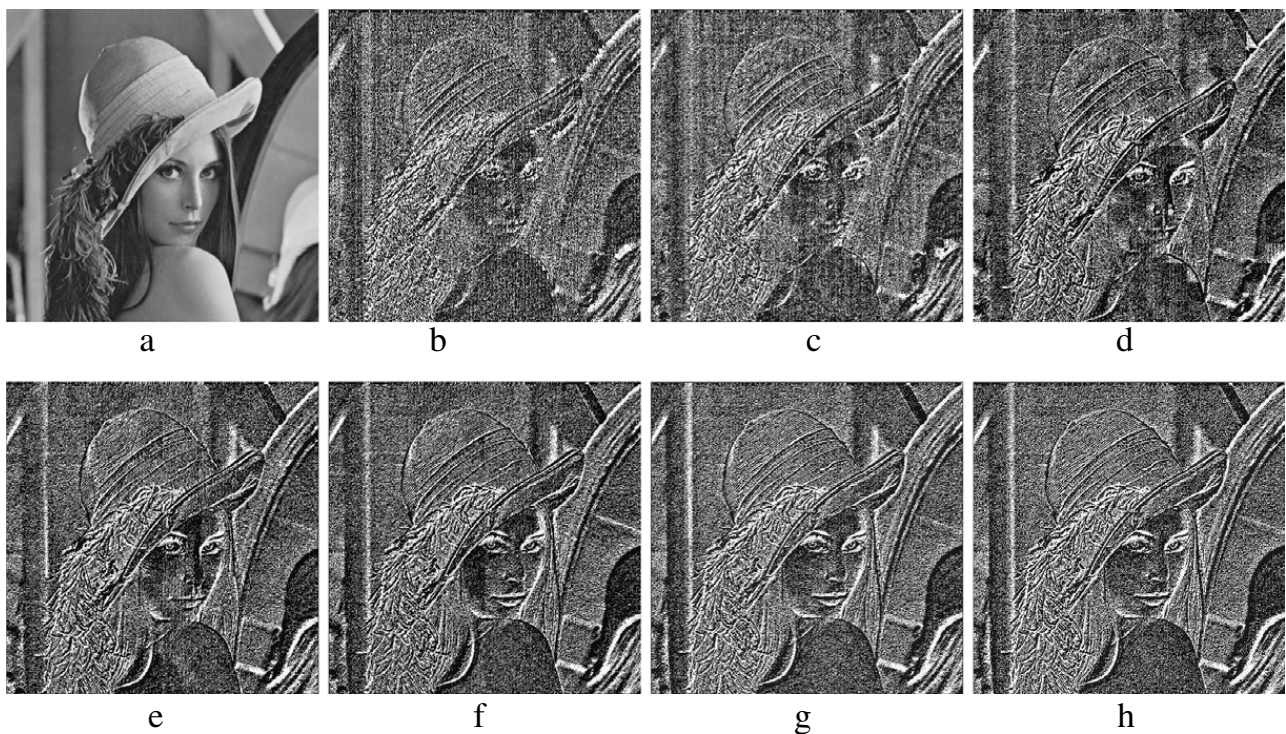


Fig. 3. Original image (a). Segmentation produced by [Algorithm 2](#) with window size 8×8 , 16×16 , 32×32 , 64×64 , 128×128 , 256×256 , and 512×512 , respectively.

6. A segmentation algorithm for contaminated images

The analysis of contaminated images is of great interest in several areas of research. For example, the reconstruction of contaminated images is relevant in image modeling ([Allende and Galbiati, 2004](#); [Vallejos and Mardesic, 2004](#)), and in general the reduction of the noise produced by interferences taking place in the processes of obtaining the physical image and of transmitting it electronically plays an important role in the literature ([Bustos, 1997](#)).

In this section, using real images, we inspect the performance of [Algorithm 2](#) to produce segmentation on a contaminated image. A numerical example is presented for an additively contaminated image previously processed in this study. The objective is to determine if [Algorithm 2](#) is able to capture the boundaries and borders existing in the original image when the entry image to [Algorithm 2](#) is an additively contaminated version of the original image.

[Fig. 4\(a\)](#) is a 10% additively contaminated version of [Fig. 3\(a\)](#). We visually observe the noise caused by the outliers. Using moving windows of sizes 8×8 , 16×16 , 32×32 , 64×64 , 128×128 , 256×256 , and 512×512 , [Algorithm 2](#) was applied to Lenna ([Fig. 3\(a\)](#)). There is an effect caused by the window size that can be observed in [Fig. 4\(b\)–\(h\)](#). There are certain vertical blocks in all processed images, and the number of vertical blocks increases as the window size increases, making a strong difference between the segmentation produced by [Algorithm 2](#) for non-contaminated images. In [Fig. 4](#), we clearly distinguish the outliers' effects. Some contours well detected by [Algorithm 2](#) seem blurred after contamination. This pattern is confirmed for a large class of contaminated images processed by [Algorithm 2](#). In both (contaminated and non-contaminated) cases the best segmentation is produced using the window size of the original image.

[Fig. 5](#) presents further results on the adequacy of robust GM and RA estimators to model images. There are three original datasets that are frequently used in the literature as benchmarks, since they have represented a variety of different image textures. These datasets were contaminated with 10% of additive noise following a zero-mean Gaussian distribution with variance 50, yielding the figures shown in the second column of [Fig. 5](#). The contaminated datasets were used as input for [Algorithm 1](#), which produced the images shown in the third, fourth and fifth columns of [Fig. 5](#). In this case LS, GM and RA estimators were used in step 1 of [Algorithm 1](#), respectively. All images show a decreased contrast, and contamination clearly appears as a grainy effect in some of them. In spite of such defects, these estimated datasets closely resemble the original images, thus suggesting that the model is adequate for a variety of situations.

The last three columns in [Fig. 5](#) present the differences between the true and estimated datasets. The better the estimation, the less the information present in these error images. Clearly the LS estimations perform worse than GM and RA estimations, and as a consequence the images corresponding to the GM and RA estimators (last two columns) retained less information than the classical version did. Also, notice that GM and RA estimations have a similar behavior. The LS estimations are clearly worse performers than the GM and RA estimations.

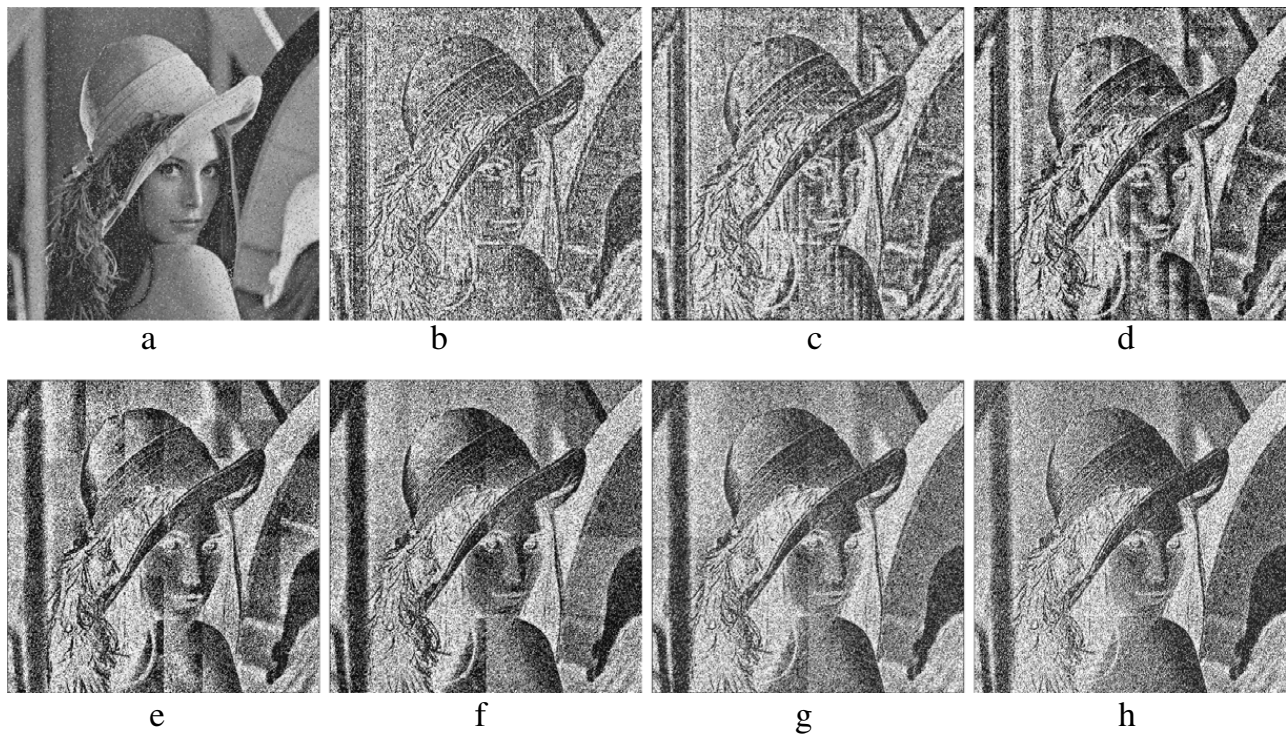


Fig. 4. (a) 10% contaminated version of Fig. 3 (a). Segmentation produced by Algorithm 2.

After experimenting with a large class of images, we recommend the use of LS estimators in [Algorithm 2](#) for segmentation, although the image looks contaminated. For filtering purposes, we support the well-known idea that robust estimation yields images closer to the original than those obtained using classical LS estimation.

To evaluate the performance of [Algorithm 2](#) with respect to other image segmentation filters, a new experiment was carried out under contamination. The input image considered here is the image shown in [Fig. 4\(a\)](#) (Lenna contaminated with 10% of additive Gaussian noise). Then [Algorithm 2](#), a Robert filter and a Sobel filter were applied to this contaminated image to observed the relative performance of the filters. The results are shown in [Fig. 6](#).

Notice from [Fig. 6](#) that the image yielded by [Algorithm 2](#) ([Fig. 6\(a\)](#)) shows more detailed patterns that are present in the original non-contaminated image ([Fig. 3\(a\)](#)). However, the segmentation produced by the Robert and Sobel filters were more affected by the additive noise. Hence [Algorithm 2](#) stands out as a good segmentation procedure when there is additive contamination.

7. An application to image inpainting

Inpainting, the technique of reconstructing small damaged portions of an image, has received considerable attention in recent years. This consists of filling in the missing areas or modifying the damaged ones in a non-detectable way for an observer not familiar with the original images. Inpainting serves a wide range of applications, such as restoration of photographs, films and paintings, and removal of occlusions, such as text, subtitles, stamps and publicity, from images. In addition, inpainting can also be used to produce special effects. Some relevant contributions in this regard were made by [Bertalmio et al. \(2000, 2003\)](#), [Oliveira et al. \(2001\)](#), [Criminisi et al. \(2004\)](#), among others.

Most inpainting methods work as follows. First, the regions of the image to be inpainted are selected, usually manually. Next, color information is propagated inward from the regions' boundaries, i.e., the known image information is used to fill in the missing areas. To produce a perceptually plausible reconstruction, an inpainting technique should attempt to continue the isophotes (lines of equal gray value) as smoothly as possible inside the reconstructed region. In other words, the missing region should be inpainted so that the inpainted gray value and gradient extrapolate the gray value and gradient outside it (see [Telea, 2004](#)). Here, we shall concentrate our attention on detecting the changes that have been done by using inpainting techniques over a certain image. In general, the changes yielded by using inpainting are visually undetectable. However, our image segmentation algorithm ([Algorithm 2](#)) applied on an inpainted image is able to highlight the original failures or missing spots existing in the original textures. Precisely, let Z be the original image having imperfections or failures. Let W be the reconstructed image by using inpainting. Then W is used as input for [Algorithm 2](#). It is expected that the image produced by [Algorithm 2](#) (Z^*) should recover the original notorious imperfections on Z . This scheme is shown in [Fig. 7](#).

[Algorithm 2](#) was applied to two images previously processed by different inpainting techniques. The first one is Lenna ([Fig. 8\(a\)](#)), reconstructed ([Fig. 8\(b\)](#)) using a method suggested by [Ballester et al. \(2001\)](#). The second one is an old picture of Abraham Lincoln ([Fig. 9\(a\)](#)), reconstructed ([Fig. 9\(b\)](#)) by an inpainting method proposed by [Oliveira et al. \(2001\)](#). In both cases

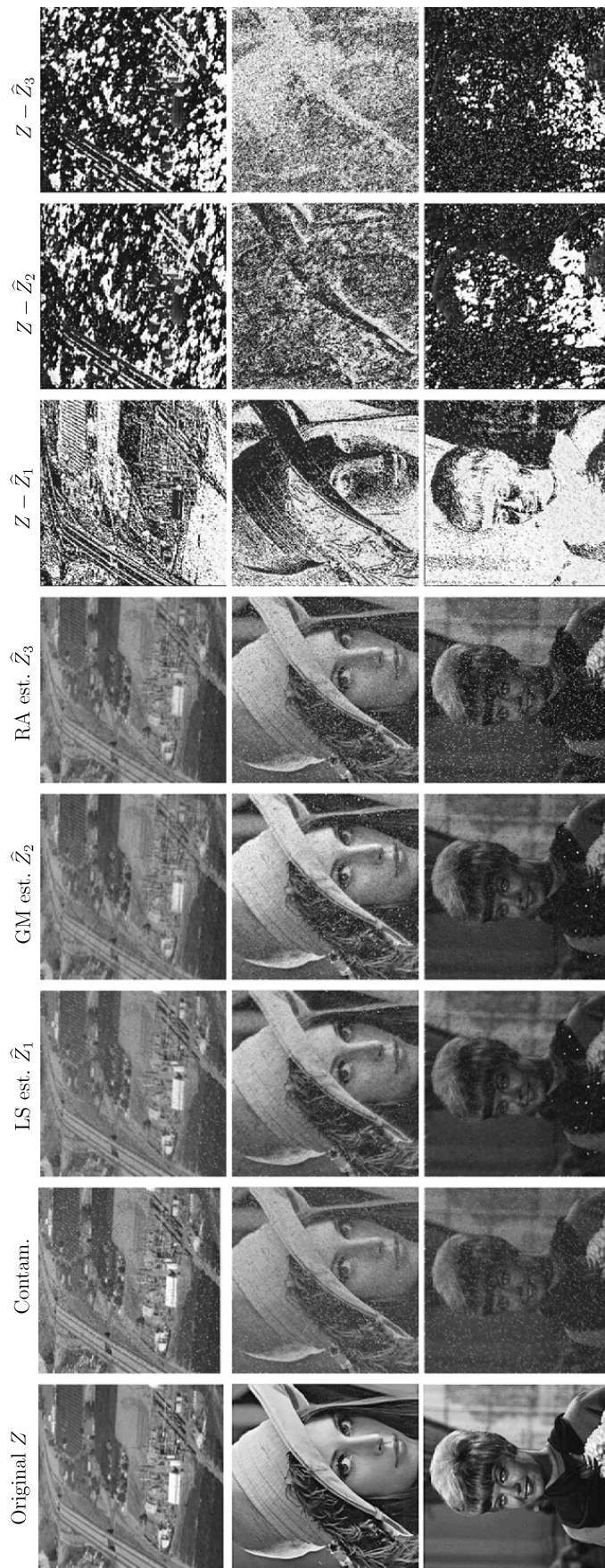


Fig. 5. Original and contaminated images, their LS, GM and RA estimators and their residuals.

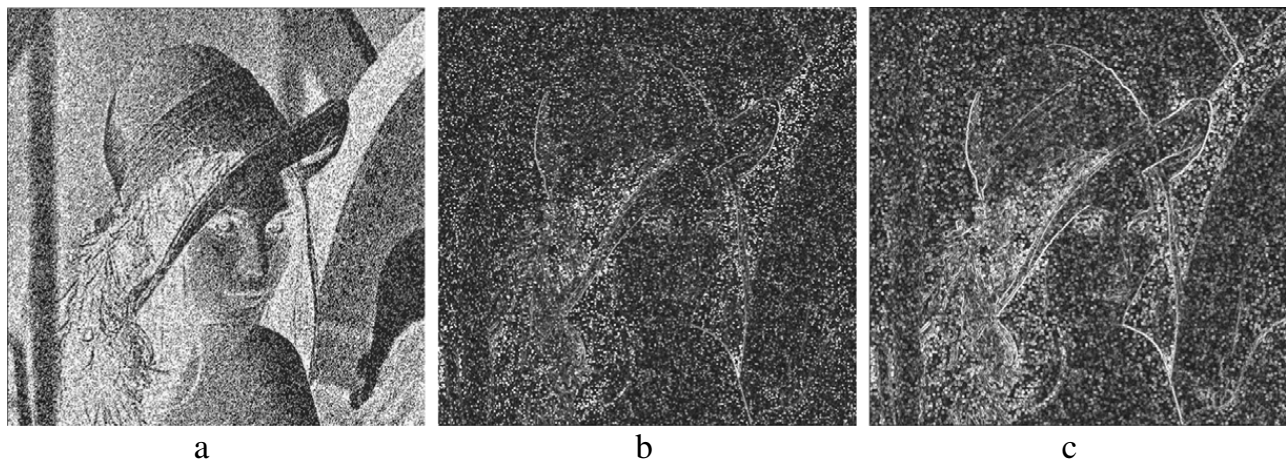


Fig. 6. (a) Output of Algorithm 2; (b) Robert filter; (c) Sobel filter.

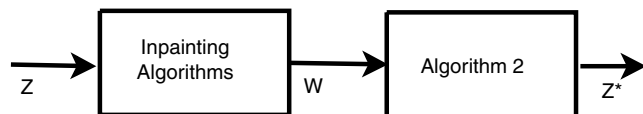


Fig. 7. Application of Algorithm 2 to recover original imperfections on inpainted images.



Fig. 8. (a) Image of Lenna with 17 holes (Ballester et al., 2001); (b) Restored image using the algorithm proposed by Ballester et al. (2001); (c) Image yielded by Algorithm 2.

the original missing spots and imperfections are not detectable by simple inspection. However, in both cases the residual autoregressive images yielded by Algorithm 2 (Figs. 8(c) and 9(c)) recover the spots and lines present in the original textures. The results obtained in these examples suggest that Algorithm 2 can be satisfactorily used to recover certain patterns present on images that have been previously reconstructed by inpainting techniques.

8. Final comments

In this paper, we have introduced a new algorithm to perform image segmentation. The foundations of this algorithm are random field theory and robustness for spatial autoregressive processes. In the light of the examples shown in Sections 5 and 6, we conclude that our algorithm is able to highlight the borders and contours of a large class of images. The LS estimation looks to be appropriate in this framework. On the other hand, and as is known, robust estimation of spatial AR processes is suitable for image filtering. Images generated from robust models are closer to the original ones.

The examples presented in Section 7 suggest that Algorithm 2 can be used to recover patterns in images previously processed. Algorithm 2 could also be used in astronomy to find patterns on images in which it is hard to detect clear trends and regularities, for example, images taken from space, where it is of interest to find regions with certain patterns that can be explored later on in detail in an observatory. Another field of eventual application of Algorithm 2 is surface defect detection.

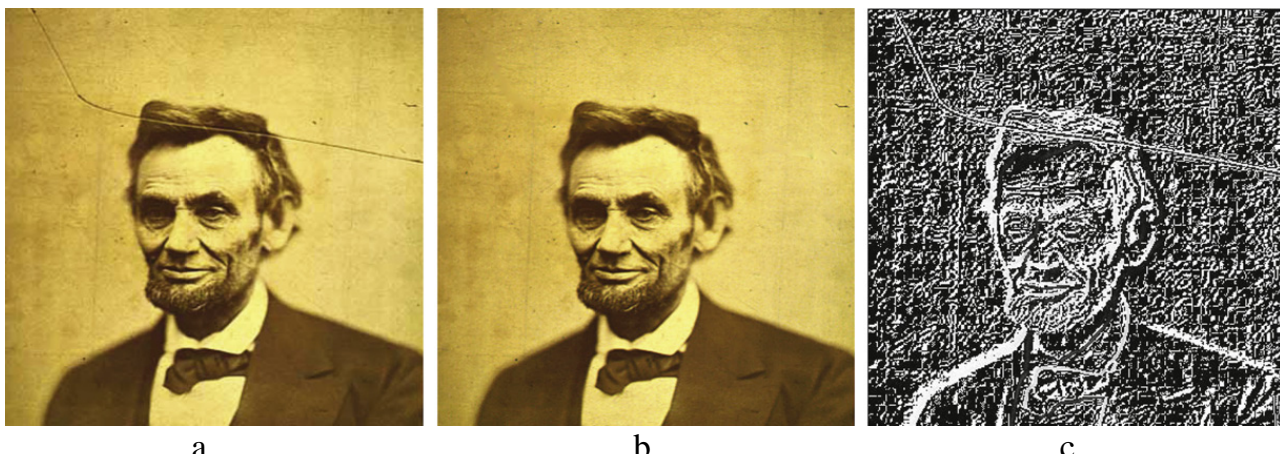


Fig. 9. (a) An 1865 photograph of Abraham Lincoln taken by Alexander Gardner (courtesy of Wing Yung and Ajeet Shankar from Harvard University); (b) Restored image using the algorithm proposed by Ballester et al. (2001); (c) Image yielded by Algorithm 2.

Several texture analysis techniques have been suggested in the literature; a recent review in this respect was written by Xie (2008).

We now outline future lines of research.

We view the work described in this paper as only the beginning of a large project with several open problems to be tackled in the future. The application of Algorithm 2 to satellite images seems to be a challenging problem. It is well known that in the acquisition process these images are contaminated or blurred by different types of noise (shift level, speckle, or other). The performance of Algorithm 2 in this context is an interesting problem to be explore. The effect of considering non-causal and semi-causal prediction windows in the spatial AR model, with different window sizes, is also an open issue to be addressed in future research.

Acknowledgements

We thank an associate editor and the referees for helpful comments and suggestions. The first author was supported by Secyt-UNC grant (05/B412), Argentina. The second author was partially supported by Fondecyt grant 11075095, Chile.

References

- Allende, H., Galbiati, J., Vallejos, R., 2001. Robust image modeling on image processing. *Pattern Recognition Letters* 22, 1219–1231.
- Allende, H., Galbiati, J., 2004. A non-parametric filter for digital image restoration, using cluster analysis. *Pattern Recognition Letters* 25, 841–847.
- Ballester, C., Caselles, V., Verdera, J., Bertalmio, M., Sapiro, G., 2001. A variational model for filling-in gray level and color images. In: Eighth IEEE International Conference on Computer Vision, 2001. ICCV 2001. Proceedings, vol. 1, pp. 10–16.
- Baran, S., Pap, G., Van Zuijlen, M.C.A., 2004. Asymptotic inference for a nearly unstable sequence of stationary spatial AR models. *Statistics & Probability Letters* 69, 53–61.
- Basu, S., Reinsel, G., 1993. Properties of the spatial unilateral first-order ARMA model. *Advances in Applied Probability* 25, 631–648.
- Bertalmio, M., Sapiro, G., Caselles, V., Ballester, C., 2000. Image inpainting. In: Proc. ACM Conf. Comp. Graphics, SIGGRAPH, pp. 417–424.
- Bertalmio, M., Sapiro, G., Vese, O., 2003. Simultaneous structure and texture image inpainting. In: Proc. Conf. Comp. Vision Pattern Rec., Madison, WI.
- Besag, J., 1974. Spatial interaction and the statistical analysis of lattice systems (with discussion). *Journal of the Royal Statistical Society Series B* 55, 192–236.
- Bustos, O., Yohai, V., 1986. Robust estimates for ARMA models. *Journal of the American Statistical Association* 81, 55–68.
- Bustos, O., 1997. Robust Statistics in SAR image processing. *ESA-SP* 407, 81–89.
- Bustos, O., Ruiz, M., Ojeda, S., Vallejos, R., Frery, A., 2009a. Asymptotic behavior of RA-estimates in autoregressive processes. *Journal of Statistical Planning and Inference* 139, 3649–3664.
- Bustos, O., Ojeda, S., Vallejos, R., 2009b. Spatial ARMA models and its applications to image filtering. *Brazilian Journal of Probability and Statistics* 23, 141–165.
- Cariou, C., Chehdi, K., 2008. Unsupervised texture segmentation/classification using 2-D autoregressive modeling and the stochastic expectation–maximization algorithm. *Pattern Recognition Letters* 29, 905–917.
- Chang, I., Tiao, G.C., Chen, C., 1988. Estimation of time series parameters in the presence of outliers. *Technometrics* 3, 193–204.
- Chen, C., Lui, L., 1993. Joint estimation of model parameters and outliers in time series. *Journal of the American Statistical Association* 88, 284–297.
- Choi, B., 2000. On the asymptotic distribution of mean, autocovariance, autocorrelation, crosscovariance and impulse response estimators of a stationary multidimensional random field. *Communications in Statistics. Theory and Methods* 29, 1703–1724.
- Criminisi, A., Perez, P., Toyama, K., 2004. Region Filling and object removal by exemplar-based image inpainting. *IEEE Transactions on Image Processing* 13, 1200–1212.
- Cullis, B.R., Glesson, A.C., 1991. Spatial analysis of field experiments—an extension to two dimensions. *Biometrics* 47, 1449–1460.
- Francos, J., Friedlander, B., 1998. Parameter estimation of two-dimensional moving average random fields. *IEEE Transaction on Signal Processing* 46, 2157–2165.
- Fox, A.J., 1972. Outliers in time series. *Journal of the Royal Statistical Society Series B* 34, 350–363.
- Grondona, M.R., Crossa, J., Fox, P.N., Pfeiffer, W.H., 1996. Analysis of variety yield trials using two-dimensional separable ARIMA processes. *Biometrics* 52, 763–770.
- Guo, J., Billard, L., 1998. Some inference results for causal autoregressive processes on a plane. *Journal of Time Series Analysis* 19, 681–691.
- Guyon, X., 1982. Parameter estimation for a stationary process on a d -dimensional lattice. *Biometrika* 69, 95–105.
- Guyon, X., 1993. Champs Aléatoires Sur un Réseau Modélisations. In: Statistique et Applications. Masson, Paris.

- Guyon, X., 1995. Random fields on a network. In: Modeling, Statistics and Applications. Springer, Berlin.
- Haining, R.P., 1978. The moving average model for spatial interaction. Transactions and Papers, Institute of British Geographers (N.S.) 3, 202–225.
- Illig, A., Truong-Van, B., 2006. Asymptotic results for spatial ARMA Models. Communications in Statistics. Theory and Methods 35, 671–688.
- Jain, A.K., Murty, M.N., Flynn, P.J., 1999. Data clustering: a review. ACM Computing Surveys 31, 264–323.
- Kashyap, R., Eom, K., 1988. Robust images techniques with an image restoration application. IEEE Transactions on Acoustics, Speech and Signal Processing 36, 1313–1325.
- Martin, R.D., 1980. Robust estimation of autoregressive models. In: Brillinger, D.R., Tiao, G.C. (Eds.), Direction in Time Series. Institute of Mathematical Statistics, Haywood, CA.
- Martin, R.J., 1996. Some results on unilateral ARMA lattice processes. Journal of Statistical Planning and Inference 50, 395–411.
- Ojeda, S.M., Vallejos, R.O., Lucini, M., 2002. Performance of RA estimator for bidimensional autoregressive models. Journal of Statistical Simulation and Computation 72, 47–62.
- Oliveira, M., Bowen, B., Mackenna, R., Chang, Y., 2001. Fast digital image inpainting. In: Proceedings of the International Conference on Visualization, Imaging and Image Processing, VIIP 2001, Marbella, Spain.
- Telea, A., 2004. An image inpainting technique based on the fast marching method. Journal of Graphics Tools 9, 23–34.
- Tjostheim, D., 1978. Statistical spatial series modelling. Advances in Applied Probability 10, 130–154.
- Tsay, R.S., Peña, D., Pankratz, A.E., 2000. Outliers in multivariate time series. Biometrics 87, 789–804.
- Vallejos, R., Mardesic, T., 2004. A recursive algorithm to restore images based on robust estimation of NSHP autoregressive models. Journal of Computational and Graphical Statistics 13, 674–682.
- Vallejos, R., Garcia-Donato, G., 2006. Bayesian analysis of contaminated quarter plane moving average models. Journal of Statistical Computation and Simulation 76, 131–147.
- Whittle, P., 1954. On stationary processes on the plane. Biometrika 41, 434–449.
- Xia, Y., Feng, D., Zhao, R.C., 2006. Morphological multifractal estimation for image segmentation. IEEE Transactions on Image Processing 15, 614–623.
- Xie, X., 2008. A review of recent advances in surface defect detection using texture analysis techniques. Electronic Letters on Computer Vision and Image Analysis 7, 1–22.